

# Enhancement of high strain rate superplastic elongation of a modified 5154 Al by subsequent rolling after equal channel angular pressing

Kyung-Tae Park <sup>a,\*</sup>, Hang-Jae Lee <sup>a</sup>, Chong Soo Lee <sup>b</sup>,  
Won Jong Nam <sup>c</sup>, Dong Hyuk Shin <sup>d</sup>

<sup>a</sup> Division of Advanced Materials Science & Engineering, Hanbat National University, Taejon 305-719, Republic of Korea

<sup>b</sup> Department of Materials Science & Engineering, POSTECH, Pohang 790-784, Korea

<sup>c</sup> School of Advanced Materials Engineering, Kookmin University, Seoul 136-702, Korea

<sup>d</sup> Department of Metallurgy and Materials Science, Hanyang University, Ansan 425-791, Korea

Received 16 January 2004; received in revised form 27 May 2004; accepted 1 June 2004

## Abstract

Subsequent rolling after equal channel angular pressing (ECAP) resulted in a considerable enhancement of the high strain rate superplastic elongation of a modified 5154 Al alloy, compared to that of the alloy subjected to the identical ECAP strain without rolling. The mechanical data revealed that the deformation of the former was governed by grain boundary sliding but that of the latter was dominated by viscous glide.

© 2004 Acta Materialia Inc. Published by Elsevier Ltd. All rights reserved.

*Keywords:* Aluminum alloy; Superplasticity; Equal channel angular pressing; Rolling

## 1. Introduction

It has been well-documented that grain refinement in some experimental or commercial Al alloys down to the submicrometer level (i.e. ultrafine grain (UFG) size) by equal channel angular pressing (ECAP) results in high strain rate superplasticity (HSRS) [1,2]. The number of ECAP passage and the selection of ECAP route are the critical factors for achieving the optimum microstructure for the maximum HSRS elongation in terms of the grain size and grain boundary misorientation. The previous investigation [3] revealed that 8 passes of

ECAP with route  $B_c$  through a die yielding an effective strain of  $\sim 1$  per a single pass optimized the UFG microstructure for the maximum HSRS elongation. However, ECAP is a relatively complicated multi-step process including sample rotation between passages. In addition, most ECAP die available at present is designed to fabricate bars with either circular or square cross-sections, being difficult to fabricate sheets or plates which are the most widely used material shape in the industrial field. To overcome these deficiencies of ECAP, it is of interest to attempt the combined process of ECAP and conventional rolling. This process is expected not only to fabricate UFG sheets but also to reduce the number of ECAP passage. In this regard, Akamatsu et al. [4] examined the effect of rolling after ECAP on the HSRS behavior of the experimental Al–3Mg–0.2Sc (in wt.%) alloy. They reported that rolling after ECAP neither

\* Corresponding author. Tel.: +82-428-211-243; fax: +82-428-211-592.

E-mail address: [ktpark@hanbat.ac.kr](mailto:ktpark@hanbat.ac.kr) (K.-T. Park).

degraded nor improved the HSRS elongation (Fig. 3 in Ref. [4]). By contrast, the present authors applied this process to a commercial Al alloy, and observed that rolling after ECAP resulted in a considerable enhancement of the HSRS elongation. In this paper, the enhancement of the HSRS elongation of a commercial Al alloy fabricated by ECAP and subsequent rolling is discussed by referring the deformation mechanisms analyzed from the mechanical data.

## 2. Experimental

A modified 5154 Al alloy was used in the present investigation. In general, the 5154 Al alloy contains 0.15–0.30 wt.% Cr. But, in this study, Sc was added instead of Cr while other alloying elements were added to the level specified for the 5154 Al alloy. This compositional modification was made under consideration that Sc is the strongest microstructure stabilizer among Al alloying elements [5,6]. After casting, the ingot was homogenized (703 K for 24 h + 793 K for 12 h), furnace cooled and then extruded into a billet of 55 mm (width) × 25 mm (thickness) at 673 K. The final chemical composition is shown in Table 1. The extruded billet was further solution-treated at 863 K for 1 h: the incipient melting temperature of the present alloy was measured as 868 K by differential scanning calorimetry.

After machining the cylindrical sample of  $\varnothing 10$  mm × 130 mm from the solution-treated billet, ECAP was conducted at 473 K with a die yielding an effective strain of  $\sim 1$  by a single pass. Since grain refinement by ECAP is usually saturated around an effective strain of  $\sim 4$  [7,8], ECAP was performed up to 4 passes (an accumulated strain of  $\sim 4$ ) with route  $B_c$ . After ECAP, cold rolling was carried out up to a total reduction of

85% with 0.2 mm reduction per rolling pass. The sectioning of the ECAPed segment for subsequent rolling is schematically described in Fig. 1. Rolling was conducted on the sectioned sample such that the X, Y and Z planes corresponded to the planes perpendicular to the rolling (RD), transverse (TD) and normal (ND) directions, respectively, as shown in Fig. 1.

For superplastic deformation, tensile specimens with a gage length of 8 mm were machined from both as-ECAPed bars and rolled sheets. The thickness of tensile specimens was 2 mm except those taken from sheets rolled to a total reduction of 85% (in this case, 1 mm). Tensile tests were carried out at the initial strain rates of  $1 \times 10^{-4}$ – $5 \times 10^{-1} \text{ s}^{-1}$  and temperature of 723 K on an Instron machine operating at a constant rate of cross-head displacement: the preliminary test revealed that 723 K was the optimum HSRS temperature for the present alloy. All the tests were performed in a three-zone furnace in air. The testing temperature was controlled within  $\pm 3$  K. Microstructures were examined by transmission electron microscopy (TEM, JEOL 2010 with 200 kV) on the Y plane for the ECAPed sample without rolling, and the Z plane for the sample fabricated by ECAP and subsequent rolling.

## 3. Results and discussion

Fig. 2a and b show TEM microstructure taken from the Y plane of the 4 passes ECAPed sample, and that taken from the Z plane of the 4 passes ECAPed sample with subsequent rolling (70% reduction), respectively: hereafter, the former and latter samples are denoted as the ECAP and ECAP+CR(70%) samples, respectively. While the ECAP sample exhibited a nearly equiaxed UFG structure of 0.2–0.4  $\mu\text{m}$ , the microstructure of

Table 1  
Chemical composition (wt.%) of the present modified 5154 Al

Mg	Sc	Fe	Si	Zn	Ti	Cu	Mn	Al
3.22	0.13	0.07	0.04	0.01	0.007	0.005	0.002	Balance

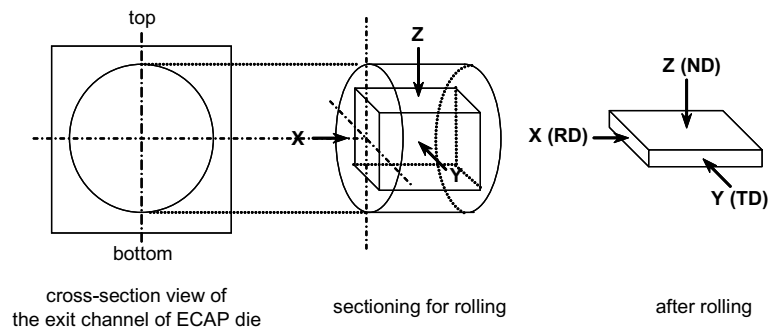


Fig. 1. Pictorial illustration showing the sectioning of the ECAPed segment for subsequent rolling.

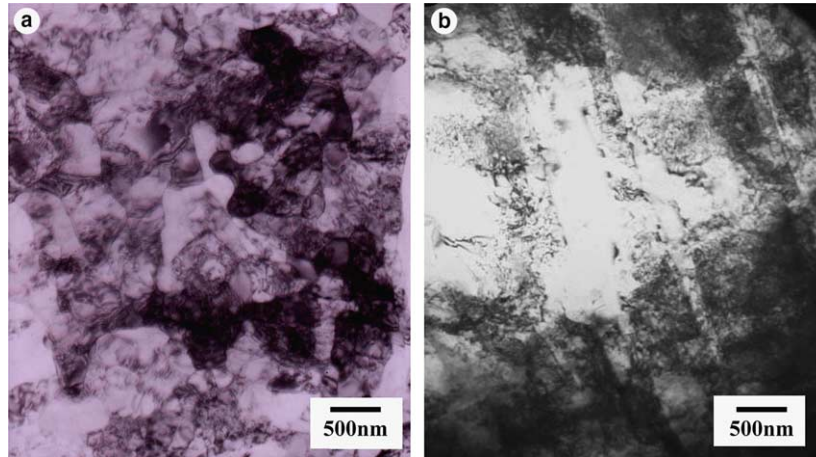


Fig. 2. TEM micrographs of (a) the ECAP sample and (b) the ECAP+CR(70%) sample of the present modified 5154 Al.

the ECAP+CR(70%) sample mainly consisted of elongated grain bands delineated by lamellar boundaries. The band width was comparable to the (sub)grain or cell size of the ECAP sample. In addition, the dislocation density at the band interior was extremely high. Being investigated at present, information on the effect of severe plastic deformation on the boundary misorientation distribution is available in the literature. For Al–3Mg–0.2Sc alloy, Akamatsu et al. [4] reported that rolling with 70% reduction after 4 passes ECAP increased the area fraction showing well-defined ring selected area diffraction pattern, indicating the dominant existence of high angle boundaries, from  $\sim 30\%$  before rolling to  $\sim 70\%$ . By comparing misorientation evolution in several Al–Mg and Al–Mn alloys fabricated by either ECAP or rolling, Mishin et al. [9] reported that there was no significant difference of misorientation evolution between ECAP and rolling at the similar strain level. Then, higher strain associated with additional rolling after ECAP is expected to develop more high angle boundaries compared to ECAP only. In addition, Apps et al. [10] addressed that the existence of coarse second phase particles accelerated the rate of development of high angle boundaries during ECAP due to plastic flow inhomogeneity. From the above previous experimental observations along with the fact that the present Al–Mg based modified 5154 Al alloy contains a fair amount of coarse second phase particles, the ECAP+CR samples are anticipated to possess higher fraction of high angle boundaries compared to the ECAP sample.

Fig. 3 shows the variation of the elongation to failure ( $e_f$ ) of the ECAP+CR samples with the rolling reduction ratio at 723 K and the initial strain rate of  $1 \times 10^{-2} \text{ s}^{-1}$ . Without rolling,  $e_f$  of the 4 passes ECAPed sample was much smaller than that of the 8 passes ECAPed sample. For the ECAP+CR samples,  $e_f$  gradually increased up to 50% reduction and it became comparable to that of the 8 passes ECAPed sample over 70%

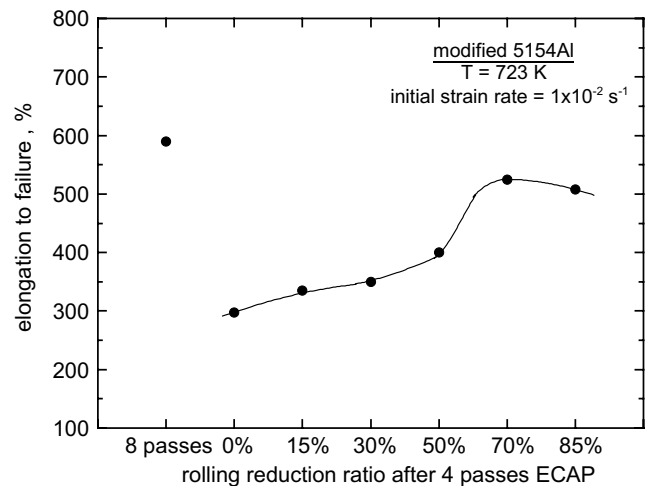


Fig. 3. The variation of the elongation to failure of the ECAP+CR samples with the rolling reduction ratio at 723 K and  $1 \times 10^{-2} \text{ s}^{-1}$ .

reduction: the appearance of the samples failed at 723 K and the initial strain rate of  $1 \times 10^{-2} \text{ s}^{-1}$  was compared in Fig. 4. A comparison of the  $e_f$  variation with the initial strain rate between the ECAP and ECAP+CR(70%) samples is shown in Fig. 5.  $e_f$  of the ECAP+CR(70%) sample was higher than that of the ECAP sample at all strain rates. It is noticeable that the maximum  $e_f$  of the ECAP+CR(70%) sample at  $5 \times 10^{-3} \text{ s}^{-1}$  (810%) was much higher than that of the 8 passes ECAPed sample at  $1 \times 10^{-2} \text{ s}^{-1}$  (590%, Fig. 3). The above findings clearly revealed that subsequent rolling, especially over 70% reduction, after ECAP was effective on enhancing the HRS elongation of the ECAPed sample. They also imply that the number of ECAP passage can be reduced by replacing it with a conventional rolling for manufacturing the HRS commercial Al alloys.

Fig. 6 shows the stress–strain rate relationship of the ECAP and ECAP+CR(70%) samples in a double

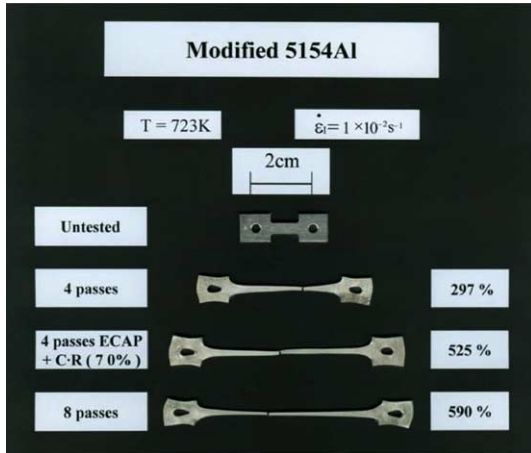


Fig. 4. Comparison of an appearance of the failed samples at 723 K and  $1 \times 10^{-2} \text{ s}^{-1}$ .

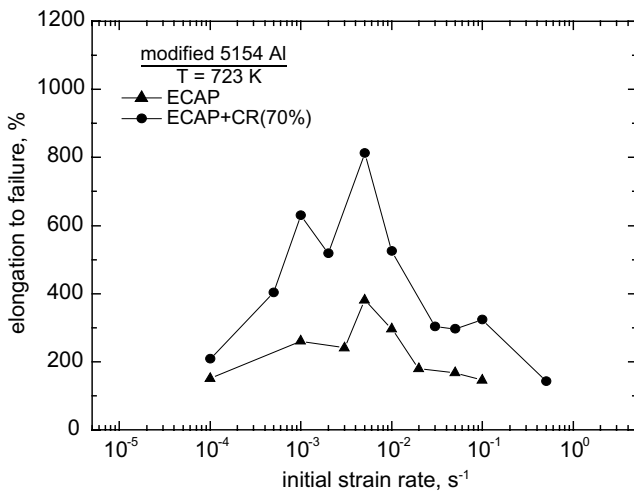


Fig. 5. Elongation to failure of the ECAP (4 passes) and ECAP (4 passes) + CR(70%) samples as a function of the initial strain rate at 723 K.

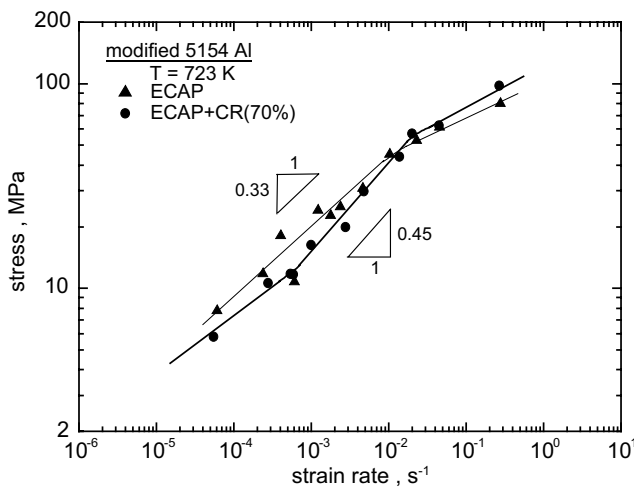


Fig. 6. A double logarithmic stress–strain rate plot of the ECAP(4 passes) and ECAP(4 passes) + CR(70%) samples at 723 K.

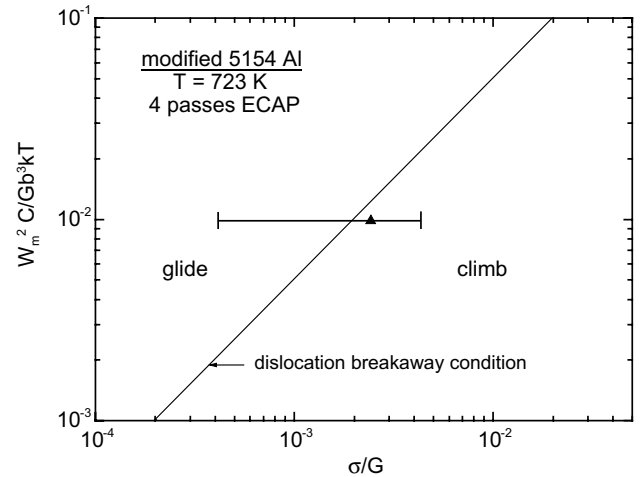


Fig. 7. The dislocation breakaway criterion which defines the dominant deformation mechanism domain for the ECAP sample under the present experimental conditions.

logarithmic scale. The ECAP + CR(70%) sample exhibited a sigmoidal curve, as typical in the superplastic materials, in which the strain rate sensitivity ( $m$ ) at the intermediate strain rates was  $\sim 0.45$ : that is, grain boundary sliding is responsible for the large HSRS elongation in the ECAP + CR(70%) sample. By contrast, except high strain rates faster than  $1 \times 10^{-2} \text{ s}^{-1}$ , the deformation behavior of the ECAP sample was characterized by  $m=0.33$ , indicating that viscous glide is a dominant mechanism. As shown in Fig. 7, the application of the dislocation breakaway model [11] which defines the dominant deformation mechanism domain also confirms that viscous glide governed the deformation of the ECAP sample at strain rates slower than  $1 \times 10^{-2} \text{ s}^{-1}$ . The detailed procedure and the values of the parameters for the construction of Fig. 7 are described elsewhere [11–13]:  $W_m$  is the binding energy between the dislocation and the solute atom,  $c$  is the solute atomic concentration,  $b$  is the Burgers vector,  $G$  is the shear modulus,  $\sigma$  is the stress, and  $kT$  has its usual meaning. In Fig. 7, the inclined line represents the transition condition between viscous glide (left side) and climb (right side) after dislocation breakaway from the solute atmospheres. The horizontal line covers the present experimental range of  $(\sigma/G)$  where the  $\sigma$  value was taken from Fig. 6. It can be seen that the observed  $(\sigma/G)$  (the closed symbol) for transition from  $m=0.2$  to  $m=0.33$  is close to the border line.

#### 4. Conclusions

1. A combined process consisting of ECAP and subsequent rolling was applied to fabricate the UFG Al alloy sheets and its effect on their HSRS elongation was examined.

2. Subsequent rolling over 70% reduction after ECAP resulted in a considerable enhancement of the HSRs elongation of the UFG modified 5154 Al alloy, compared to the alloy subjected to the identical ECAP strain without rolling. Specifically, 4 passes ECAP with 70% rolling resulted in the elongation comparable to that of the 8 passes ECAPed sample without rolling.
3. Under the present experimental conditions, grain boundary sliding was a dominant deformation mechanism for the sample fabricated by 4 passes ECAP and subsequent rolling with 70% reduction. By contrast, the deformation of the sample fabricated by only 4 passes ECAP was governed by dislocation glide.
4. The present study implies that the number of ECAP passage can be reduced by replacing it with a conventional rolling for manufacturing the HSRs commercial Al alloy sheets.

#### Acknowledgments

This work was supported by a grant (03K1501-00222) from 'Center for Nanostructured Materials Technology' under '21st Century Frontier R&D Programs' of the Ministry of Science and Technology

(MOST), Korea. One of the authors (CSL) thanks to the partial support from '2003 National Research Laboratory Programs' of the MOST, Korea.

#### References

- [1] Horita Z, Furukawa M, Nemoto M, Barnes AJ, Langdon TG. *Acta Mater* 2000;48:3633–40.
- [2] Park K-T, Hwang DY, Kim YK, Lee YK, Shin DH. *Mater Sci Eng A* 2003;341:273–81.
- [3] Komura S, Furukawa M, Horita Z, Nemoto M, Langdon TG. *Mater Sci Eng A* 2000;297:111–8.
- [4] Akamatsu H, Fujinami T, Horita Z, Langdon TG. *Scripta Mater* 2001;44:759–64.
- [5] Sawtell RR, Jensen CL. *Metall Trans A* 1990;21:421–30.
- [6] Kramer LS, Tack WT, Fernandes MT. *Adv Mater Proc* 1997;23–4.
- [7] Chang SY, Lee GK, Park K-T, Shin DH. *Mater Trans (JIM)* 2001;42:1074–80.
- [8] Kaibyshev R, Sitdikov O, Olenyov S. In: Zhu YT, et al, editors. *Ultrafine grained materials II*. Warrendale, USA: TMS; 2002. p. 65–74.
- [9] Mishin OV, Juul Jensen D, Hansen N. *Mater Sci Eng A* 2003;342:320–8.
- [10] Apps PJ, Bowen JR, Prangnell PB. *Acta Mater* 2003;51:2811–22.
- [11] Yavari P, Langdon TG. *Acta Metall* 1982;30:2182–96.
- [12] Friedel J. In: *Dislocations*. Oxford, UK: Pergamon Press; 1964. p. 351.
- [13] Bird JE, Mukherjee AK, Dorn JE. In: Brandon DG, Rosen A, editors. *Quantitative relation between properties and microstructures*. Jerusalem: Israel University Press; 1969. p. 255.